

Energy Deposition of a ZnWO₄ Thin-Film Scintillator for High-Resolution X-ray Imaging

Jaewoo Lee ^a, Ju Hyuk Lee ^a, Heon Yong Jeong ^a, Taeyun Kim ^{b,c}, Sung Oh Cho ^{a*}

^aDept. of Nuclear & Quantum Engineering, Korea Advanced Institute of Science & Technology, Daejeon, Republic of Korea, 34141

^bHANARO Utilization Division, Korea Atomic Energy Research Institute, Daejeon, Republic of Korea, 34057

^cDept. of Transdisciplinary Studies, Seoul National University, Seoul, Republic of Korea, 08826

*Corresponding author: socho@kaist.ac.kr

1. Introduction

One of the most representative fields of scintillator is high-resolution X-ray imaging. There are typically two kinds of scintillators, organic scintillators and inorganic scintillators. Inorganic scintillator has advantages of higher luminous efficiency and better linearity compared to the organic scintillator. Among various inorganic scintillators, zinc tungstate (ZnWO₄) is a promising material as a scintillator due to its high density and effective atomic number, and excellent mechanical and chemical properties [1-2]. In addition, it has relatively high light yield (~10,000 photons/MeV) [3], which can generate a significant number of photons.

The thickness of the scintillator is greatly related to image resolution [4]. In the case of thick scintillators, they generally have a mesh-grid structure, exhibiting high sensitivity. However, the grid size is limited to minimize and the scintillators suffer from low reproducibility. When thin-film scintillators are used, the sensitivity is less spread out, resulting in higher sensitivity. Powder-type thin-film scintillators are easy to fabricate and flexible, but the powder particles scattered the optical photons [5]. Despite the high spatial resolution and stability of glass-type thin-film scintillators, the fabricating method is quite complex.

In this paper, we investigate the energy deposition of a glass-type ZnWO₄ thin-film scintillator using the Monte Carlo N-Particle (MCNP) transport code. For high-resolution X-ray imaging, the system includes an X-ray tube with constant tube power. Since the generated X-ray energy spectrum varies depending on tube current and tube voltage, energy absorption will also have various values within a constant tube power. This may affect the resolution of an image, so analysis through simulation is required.

2. Methods

2.1 Geometry Construction

The high-resolution X-ray imaging system consists of an X-ray tube, a scintillator, a magnification lens, and a detector as depicted in Fig. 1. It is noteworthy that the distance between an object and a scintillator is almost zero. The simplified illustration of the X-ray tube used in the simulation is presented in Fig. 2a. The outside of the tube was sealed with glass, and the inside was set to

a vacuum atmosphere. Tungsten target and a beryllium window (Φ 1.26 cm, 0.01 cm thickness) are selected, and other detailed components as well as the dimension of tube complied with a microfocus X-ray tube model P030.24.12F100W (Petrick GmbH, Germany). The thickness of the scintillator was calculated by Eq. 1, and 3 μ m was obtained by using the known parameters.

$$t = \frac{sl}{M^2D} \quad (1)$$

where, t is the thickness of scintillator for high-resolution X-ray images, s is the detector pixel size (6.5 μ m), l is the distance between the magnification lens and the detector (21 cm), M is the magnification (8), and D is the diameter of the magnification lens (0.75 cm) in the imaging system. Therefore, the scintillator was applied in the form of a 3 μ m ZnWO₄ layer deposited on 1 mm thick quartz (Φ 15 mm). A simple description of X-rays generated from the tube incident on the scintillator is shown in Fig. 2b. The X-ray source was set as a disk.

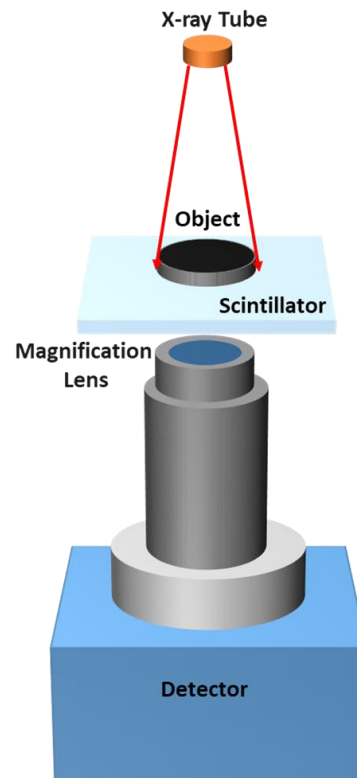


Fig. 1. An illustration of the general X-ray imaging system.

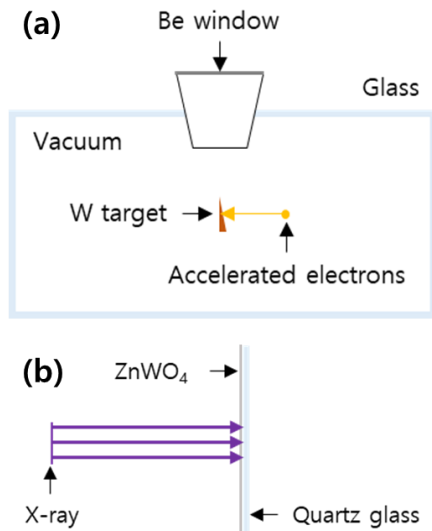


Fig. 2. Simplified construction of (a) the X-ray tube and (b) X-rays incident on the scintillator for MCNP simulation.

2.2 MCNP Simulation

The simulation was performed using the MCNP6 code developed from Los Alamos National Laboratory. The glass envelope is cylindrical ($\Phi 3$ cm), which is 6.2 cm long, 0.1 cm thickness and the density is 2.23 g/cm^3 . The density of the vacuum filled inside the glass envelope was set to 10^{-20} g/cm^3 . The W target was chosen in the shape of a truncated cylinder and was placed in the center of the tube. The position of the electron source is at a point 1 cm away from the target and is incident with a mono-energy in the direction of the target (*i.e.*, uni-direction). The energy of electrons was applied differently according to the change of tube voltage. X-rays generated by the reaction of electrons with the target pass through the Be window in the vertical direction. The collimator connected with the Be window is in the form of a truncated cone. The external environment of the X-ray tube consists of air (density of 0.001205 g/cm^3), and the tally was assigned to a position perpendicular to the direction in which the electrons were incident to collect X-rays. Using F4 tally with energy bins and “Mode P, E”, it was simulated at 10^9 NPS, and the area outside the region of interest was defined as void. For importance, photons and electrons were set to “1”, and in the void region, “0” were assigned so that no photons and electrons exist. Fig. 3a and 3b show the geometry of the defined cells.

Subsequently, further simulation was conducted for calculating the energy deposition of the scintillator. The density and thickness of ZnWO₄ film are 7.62 g/cm^3 and $3 \mu\text{m}$, respectively. The disk type of ZnWO₄ thin film is on a quartz glass substrate, whose density is 2.648 g/cm^3 . The ambient environment was set to air and the area outside the region of interest was also defined as void. The importance of photons and electrons were assigned to “1”, and “0” for external void space. For the X-ray

source, the histogram was defined to have a continuous energy distribution using “SI” and “SP” commands from the X-ray energy spectra derived above, and it has a different source distribution according to the tube voltage. The source was defined as a disk shape with the same area as the Be window and incident in uni-direction towards the scintillator. The scintillator was designated as a tally cell and energy deposition by photons and electrons was calculated using *F8 tally with “Mode P, E”. The history was repeated with 10^8 NPS. Fig. 3c presents the simulated scintillator.

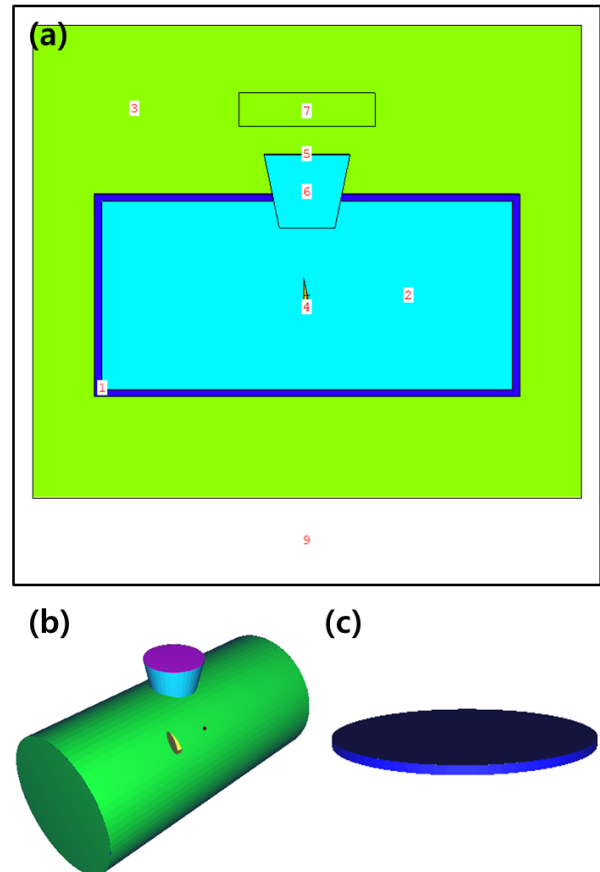


Fig. 3. (a) Defined cells simulated by MCNP, and a three-dimensional image of the simulated (b) X-ray tube and (c) ZnWO₄ thin-film scintillator.

3. Results and Discussion

3.1 X-ray Energy Spectrum

At a constant 50 W tube power, when the tube voltage is altered, the tube current also changes. Therefore, the tube current is inversely proportional to the tube voltage (Fig. 4a), which in turn changes the number of electrons incident on the target. In general, the number of incident electrons is proportional to the tube current. Fig. 4b shows the X-ray spectra derived from simulation under five conditions of tube voltage/current. Since the MCNP code provides an X-ray spectrum corresponding to one electron, the total

number of X-ray photons was obtained by multiplying the number of electrons generated by each tube current. At 20, 25, 40, and 50 kV_p, it can be seen that two W characteristic X-rays appear near about 10 keV, and such a peak could not be observed at 10 kV_p. As shown in Table I, the number of X-ray photons calculated from the simulation results shows that the number of photons increases at the higher tube voltages.

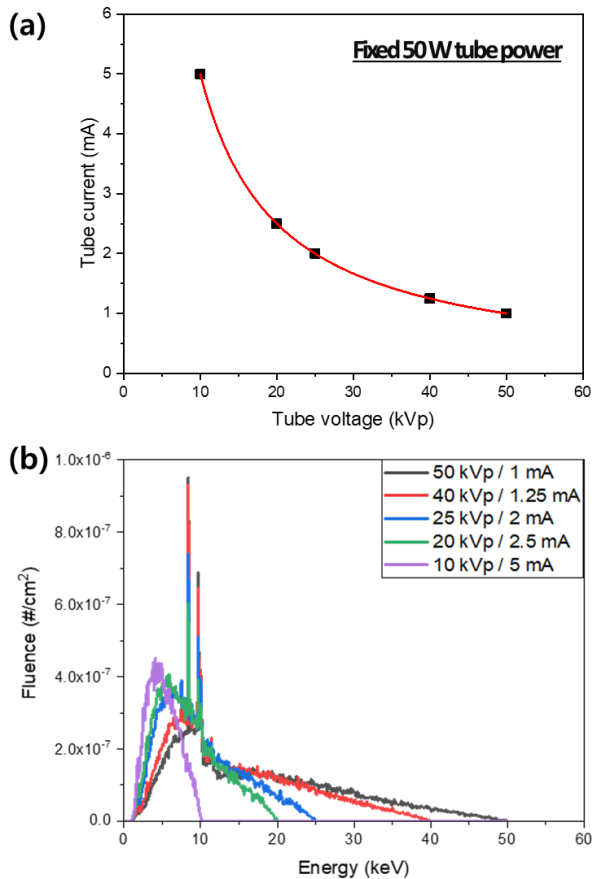


Fig. 4. (a) Relationship between tube current and tube voltage at a fixed 50 W tube power and (b) calculated X-ray energy spectra at various tube voltage/current conditions.

Table I: The number of generated X-ray photons calculated from MCNP simulation.

| Tube voltage (kV _p) | Number of photons (s ⁻¹) |
|---------------------------------|--------------------------------------|
| 10 | 1.09×10 ¹¹ |
| 20 | 1.76×10 ¹¹ |
| 25 | 1.93×10 ¹¹ |
| 40 | 2.19×10 ¹¹ |
| 50 | 2.30×10 ¹¹ |

3.2 Deposited Energy in the Scintillator

In order to obtain the energy absorption of the ZnWO₄ scintillator from the X-ray spectrum according to each tube voltage simulated previously, there is a limit to the MCNP code. Since the MCNP simulation does not reflect the behavior of visible light (*i.e.*, low-energy photons) in the scintillator, we assumed that the

more energy the scintillator absorbs, the more light it produces, resulting in higher resolution. The energy absorbed in the scintillator depending on the tube voltage is presented in Fig 5a. In the same number of particles, the most energy is absorbed when the tube voltage is 20 kV_p as shown in the red line. However, since the number of X-ray photons is different for each tube voltage, this value should be multiplied by the number of photons. When the number of photons given in Table 1 is multiplied, the total deposited energy is the highest at a tube voltage of 50 kV_p (see the blue line in Fig 5a).

Although the deposited energy is highest at 50 kV_p, the energy absorption rate decreases as the tube voltage increases as shown in the green line in Fig. 5b. It suggests that the higher energy X-rays were incident at high tube voltage and were not sufficiently absorbed in the scintillator. Therefore, we expect that high resolution can be obtained at a tube voltage of about 25 kV_p and a tube current of 2 mA in consideration of the appropriate amount of deposited energy and absorption compared to the incident. Nevertheless, since it is assumed that the image resolution is affected only by absorbed energy, it is necessary to consider various variables such as light conversion efficiency, optical scattering effect, and light acquisition using the other codes.

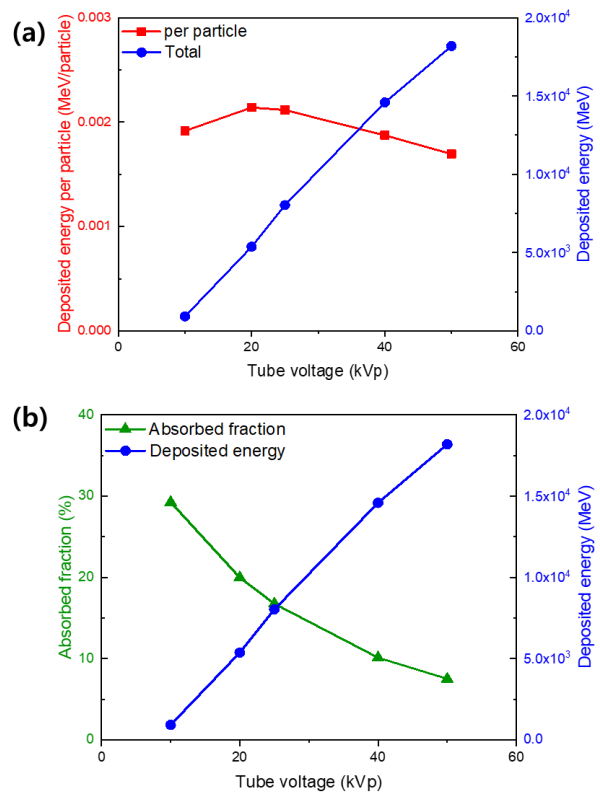


Fig. 5. (a) Energy deposition and (b) energy absorbed fraction of ZnWO₄ thin-film scintillator at various tube voltages.

4. Conclusions

The energy deposition of the ZnWO₄ thin-film scintillator was analyzed using MCNP simulation. We assumed that the deposited energy and absorption fraction would be capable of achieving high-resolution images. Since the tube current is inversely proportional to the tube voltage at a fixed tube power, the change in the X-ray spectrum generated depending on the tube voltage was identified. Accordingly, the energy deposited in the scintillator increased as the tube voltage increased, but energy absorption decreased at higher tube voltages. Therefore, it is necessary to obtain a reasonable tube voltage condition that can exhibit the best image resolution by reflecting both energy absorption and absorbed fraction. In addition to energy deposition, other optical effects also need to be investigated.

ACKNOWLEDGEMENTS

This work was supported by the National Research Foundation (No. 2020M2D8A2069727).

REFERENCES

- [1] V. B. Mikhailik and H. Kraus, Luminescence of CaWO₄, CaMoO₄, and ZnWO₄ scintillating crystals under different excitations, *Journal of Applied Physics*, Vol.97, p.083523, 2005.
- [2] P. Belli, R. Bernabei, F. Cappella, R. Cerulli, F. A. Danevich, A. M. Dubovik, S. d'Angelo, E.N. Galashov, B. V. Grinyov, A. Incicchitti, V. V. Kobychiev, M. Laubenstein, L. L. Nagornaya, F. Nozzoli, D. V. Poda, R. B. Podviyanuk, O. G. Polischuk, D. Prospero, V. N. Shlegel, V. I. Tretyak, I. A. Tupitsyna, Ya. V. Vasiliev, and Yu. Ya. Vostretsov, Radioactive contamination of ZnWO₄ crystal scintillators, *Nuclear Instruments and Methods In Physics Research A*, Vol.626-627, pp.31-38, 2011.
- [3] C. Grupen and I. Buvat (eds.), *Handbook of Particle Detection and Imaging*, Springer, New York, 2012.
- [4] Z. Yongxin, X. Honglan, D. Guohao, C. Rongchang, and X. Tiqiao, Influence of scintillators's thickness on imaging quality of lens-coupled hard X-ray imaging detector, *Nuclear Techniques*, Vol.37(7), p.6, 2014.
- [5] M. Nikl, Scintillation detectors for x-rays, *Measurement Science and Technology*, Vol.17, pp.37-54, 2006.